Eur. Phys. J. E (2009)
DOI 10.1140/epje/i2009-10514-7

THE EUROPEAN PHYSICAL JOURNAL E

Regular Article

Adhesion and membrane tension of single vesicles and living cells using a micropipette-based technique

M.-J. Colbert, A.N. Raegen, C. Fradin, and K. Dalnoki-Veress[a]

Department of Physics & Astronomy and the Brockhouse Institute for Materials Research, McMaster University, Hamilton, ON, Canada

Received 5 May 2009

Abstract. The fundamental study of the adhesion of cells to each other or to a substrate is a key research topic in cellular biophysics because cell adhesion is important to many biological processes. We report on the adhesion of a model cell, a liposome, and a living HeLa cell to a substrate measured with a novel experimental technique. The cells are held at the end of a micropipette mounted on a micromanipulator and brought into contact with a surface. The adhesion energy and membrane tension are measured directly using the deflection of the micropipette when binding or unbinding the cell from the substrate. Since the force applied on the cells is known throughout the experiment, the technique presented enables the measurement of dynamics such as changes in the adhesion, elasticity, and membrane tension with time.

PACS. 87.16.D- Membranes, bilayers, and vesicles – 87.17.Rt Cell adhesion and cell mechanics – 87.15.La Mechanical properties – 87.61.Ff Instrumentation

1 Introduction

Cell-cell and cell-matrix interactions play key roles in a range of biological processes. As a result, studies of cell adhesion have great potential for impact on health-related research. For example, the implant industry is interested in gaining a better understanding of how cells interact with the materials used for implants in order to enhance their performance [1]; and modification of cellular adhesion properties is thought to be crucial in trying to combat metasticization of cancers [2,3].

Seminal studies by Evans and co-workers have resulted in the introduction of several micropipette-based approaches to probe the adhesion between two cells or between a cell and a substrate [4–8]. One approach pioneered by this group consisted of using the micropipette to apply a variable suction pressure on a vesicle in contact with a surface. A second approach utilized a cell or vesicle itself as a force transducer in order to measure the *rupture force* —the force required to break the adhesion [7,8]. In this case, the cell was treated as a spring whose stiffness can be tuned by adjusting the suction pressure in the micropipette used to hold it [7–10]. More recently, Brochard-Wyart and co-workers further extended this methodology to obtain the adhesion energy by measuring the rupture force required to remove the cell from the contact patch [11,12].

The goal of the work presented here is twofold: to provide a precise and *direct* measurement of these physical properties of cells, and to enable the study of changes in those properties with time (*i.e.* adhesion, elasticity, and membrane tension, etc.). Such *dynamical* measurements are possible because we obtain the force and displacement during the entire course of the experiment. Furthermore, the method must be applicable to living cells. We chose a micropipette-based force transducer for the experiments. The force measurements are direct as they are based simply on the measurement of the micropipette deflection (MD). The membrane tension, and the adhesion energy is analyzed based on the point of rupture and using 2 different models based on the force balance which provide *dynamic information*. The different methods give similar results, thus validating our approach. Here we first focus on simple lipid vesicles in order to establish the validity of the MD methodology. Secondly, we present results on living cells. To the best of our knowledge these are the first adhesion measurements that have both a high force resolution and can follow dynamics of living cells.

2 Experiment

2.1 Micropipette deflection apparatus

The adhesion experiment we developed was inspired by earlier measurements by Yeung and co-workers on the strength of polymer-induced flocs [13] and a study by Francis and coworkers on red blood cells and amoebae [14]. In our MD experiments a pipette was pulled and bent into an L-shape with a length three orders of magnitude

[a] e-mail: dalnoki@mcmaster.ca

Published online: 24 September 2009

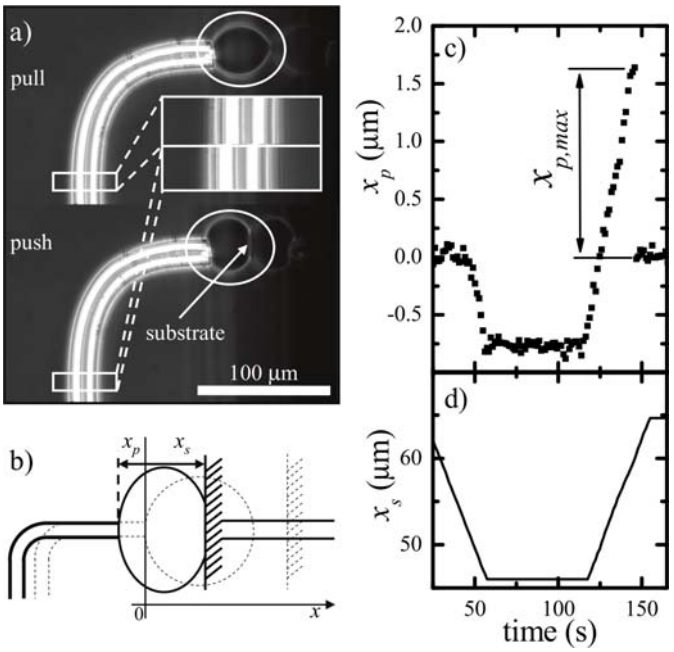

Fig. 1. (a) Image of the vesicle and its reflection on the substrate during a binding/unbinding cycle, the deflection of the pipette is clearly visible in the enlarged inset. (b) Schematic of the experiment showing the positions prior to contact between the substrate and vesicle (dashed line), and after compression (solid lines). Displacements are measured with respect to the zero force position of the pipette. Pipette (c) and substrate (d) displacement during a binding/unbinding cycle as a function of time.

larger than its diameter ($\sim 10\,\mu$m) so that the deflection of the pipette can be used directly as a force transducer. The chamber containing the vesicle was mounted atop an inverted microscope placed on an anti-vibration table (Halcyonics MOD-1). A three-axis micro manipulator (Burleigh, PCS5600) was mounted such that it can hold the micropipette inside the chamber. A small constant negative pressure inside the pipette relative to the chamber was applied and controlled by changing the height of a water reservoir. The substrate was fixed to a motorized translation stage (Newport MFN25cc), which was attached to the microscope such that the substrate is inside the chamber opposite the micropipette. The substrate, pipette and vesicle were visible with the microscope as shown in Figure 1. The substrate was tilted so that the reflection of the vesicle was visible. This is a significant advantage because it facilitates the analysis of the contact region geometry. Displacements of the substrate and the pipette were measured using cross-correlation image analysis, offering a precision of $\sim 0.1\,\mu$m.

2.2 Sample preparation

Vesicles were prepared from neutral 16:0-18:1 PC (1 - Palmitoyl - 2 - Oleoyl - sn - Glycero - 3 - Phosphocholine) (Avanti Polar Lipids) in chloroform, and formed by electroformation in an aqueous sucrose solution (0.2 M) [15]. To deflate the vesicle slightly, thereby making the membrane less taught, the osmotic pressure was adjusted by dilution of the dispersion with an equal part aqueous 0.2 M sodium chloride. The final dispersion containing the vesicles was transferred to the measurement chamber. The vesicles studied had a typical diameter ranging from 30 to 60 μm. The Si substrates were cleaned with methanol, and treated in a UV ozone chamber for one hour prior to sputter coating a ~ 200 nm gold layer. The substrate was glued on a glass rod for mounting to the motorized translation stage. Prior to use the substrate was rinsed with methanol, followed by Milli-Q water.

2.3 Force calibration

In order to make direct measurements, the pipette was calibrated through the application of a viscous force on a sphere fixed to the tip of the pipette. The chamber was filled with a viscous aqueous solution of sucrose (6.0 M). A polymer microsphere ($\sim 222\,\mu$m diameter, Duke Scientific) was held by the micropipette via suction. The chamber was moved with speed, v, causing viscous drag of the liquid on the bead. This was repeated with and without the bead in order to subtract the contribution from the pipette. Using Stokes' relation we balance the viscous drag force with the pipette displacement: $6\pi r\eta v = k\Delta d$, where k is the spring constant of the pipette, Δd is the difference between the equilibrium position of the pipette with the bead and without the bead under flow, r is the radius of the bead, and η is the viscosity of the liquid. A plot of the viscous force *versus* Δd for 10 flow velocities was obtained with the slope yielding the spring constant k (data not shown).

3 Results and discussion

3.1 Adhesion and membrane tension of lipid vesicles

Figure 1(c) and (d) show plots of the pipette deflection, x_p, and the substrate position, x_s, as a function of time during a typical experiment. The speed at which the substrate is moved is set to $0.5\,\mu$m/s. As the substrate is moved towards the vesicle, initially there is no change in the pipette position, until contact is made and a force on the vesicle is apparent as a deflection of the pipette. The substrate is moved further, compressing the vesicle and resulting in a negative pipette deflection. In order to ensure that the water between the surface and the membrane had evacuated and that adhesion occurred, the substrate was kept stationary for approximately 60 s and no change in the force is observed during this time. Subsequently the substrate motion is reversed and eventually the vesicle is under tension —held at one side by the pipette and the other by the adhesion forces at the substrate contact patch. At the point of rupture, the vesicle detaches from the interface which is clear from the sudden drop in the pipette position to zero. For the example shown in Figure 1(c) and (d), the pipette had a spring constant, $k = (12.7 \pm 0.5)\,\mathrm{nN}/\mu\mathrm{m}$

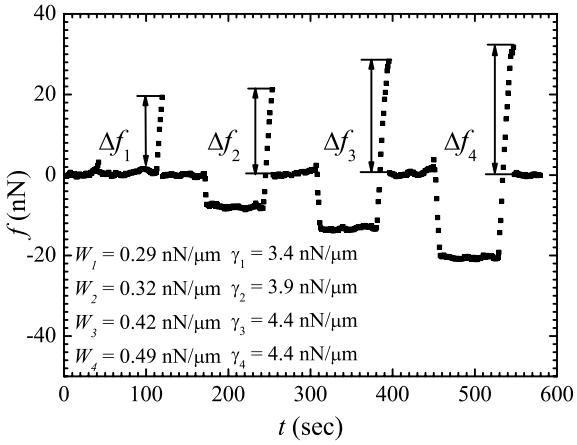

Fig. 2. Force applied by the pipette on a vesicle adhered to the surface as a function of time for 4 push/pull sequences. The adhesion energy W_i and membrane tension γ_i are shown as calculated from the rupture force.

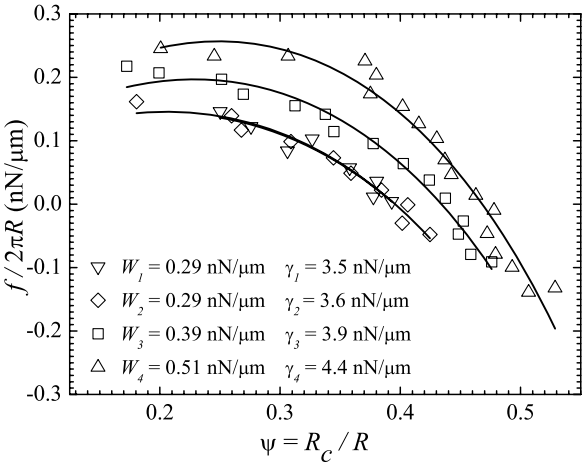

Fig. 3. The force as a function of the contact radius (scaled to the equatorial radius R) for the 4 push/pull cycles shown in Figure 2. The lines correspond to the best fit of the BWdG model with fitting parameters W_i and γ_i.

and the vesicle had a diameter of $(15 \pm 1)\,\mu$m. The maximum observed displacement of the pipette $x_{p,\max}$ was $(1.6 \pm 0.1)\,\mu$m, which corresponds to a rupture force of $f_r = kx_{p,\max} = (20 \pm 2)\,$nN.

Our MD-based rupture force measurement has a precision of $\sim 10\%$, which compares favorably with other micropipette techniques (for example $\sim 20\%$ for the microaspiration technique [16], and $\sim 40\%$ when using a vesicle as the transducer [7]). By adjusting the length and diameter of the pipette, the spring constant can be tuned to the desired force sensitivity. As shown in Figure 2, this type of binding/unbinding experiment can be repeated multiple times with the same substrate and vesicle.

In order to measure the adhesion energy and membrane tension, we use a model, applicable to vesicles, that was developed by Brochard-Wyart and de Gennes (BWdG model) [11]. Here we repeat the main points as they apply to our system. An equilibrium can be assumed between the force applied by the pipette, the surface tension and the bulk pressure. This condition is valid along the entire contour of the vesicle. Solving the force balance equation at the apex of the vesicle and at the contact point,

$$\frac{f}{2\pi R} = \gamma \frac{\psi \sin\theta_E - \psi^2}{1 - \psi^2}\,, \qquad (1)$$

where R_c is the radius at the contact, R is the equatorial radius, and $\psi = R_c/R$. Both R and R_c are measured directly from the images by fitting to the contour of the membrane. In analogy with a liquid drop, we use the Young-Dupré equation to determine the adhesion energy, $W = \gamma(\cos\theta 1)$. The combination of these two expressions for small contact angles leads to an expression of the adhesion energy that is dependent on the maximum sustainable force, $W = f_r/\pi R$, where R is the equatorial radius adopted by the vesicle at the moment of unbinding [11]. From this expression, we found an unbinding energy of $(0.27 \pm 0.04)\,$nN/μm. This value ranges from 0.3 to 0.5 nN/μm for the different cycles shown (see Fig. 2).

The membrane tension, γ, is also accessible through the Young-Dupré equation, $W = \gamma(1 - \cos\theta_E)$, with W measured from the rupture force measurement. The contact angle, θ_E, can be measured from the images or, as we did, by evaluating the value of ψ when $f = 0$ ($\theta_E = 0.41$, 0.41, 0.44, and 0.48, respectively). The values of γ calculated as such are also shown in Figure 2. Note that the adhesion increases with increasing compression, this may be due to establishing better contact under a higher load.

One of the main advantages of the MD measurement is that information regarding both elasticity and adhesion can be obtained during the *entire attachment or peeling process* (*i.e.* not only from the rupture force); thereby making it possible to observe changes in living cells as they respond to stimuli. Note that equation (1) also provides the dynamic values of the membrane tension in terms of experimentally determined quantities (*i.e.* changes in γ can be measured because the data is obtained during the binding/unbinding cycle, not only at the rupture point). The force balance of the interfacial tensions at the triple point fixes the contact angle. As expected, the contact angle was observed to be constant during each cycle (θ_E it is set by the Laplace pressure in the pipette if W is constant). This was confirmed by direct measurement of the angle from images taken throughout the experiment. Combining the Young-Dupré equation and equation (1) yields an expression of $f/2\pi R$ as a function of ψ with the only free parameters being the adhesion energy and membrane tension. In Figure 3 we show the fit of the model to the experimental data as well as the values obtained for W and γ. We note that, though in this case the system was chosen such that W and γ do not vary with time, the measurements are *dynamic* and at any point these parameters can be obtained as a function of time.

The validity of the dynamical measurements facilitated by the MD technique and the BWdG model can be verified by comparing the adhesion energies and membrane tension obtained in Figure 3 with those obtained from the

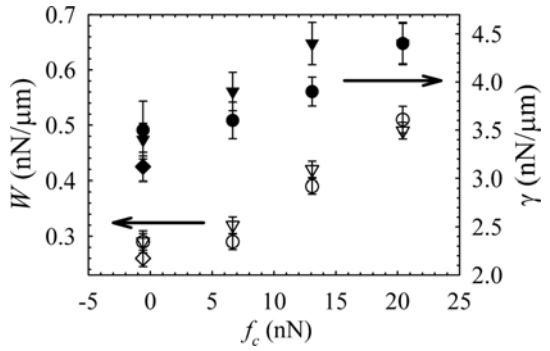

Fig. 4. Comparison between the adhesion energy (open symbols) and the membrane tension (solid symbols) obtained dynamically (circles) and from the rupture force (triangles) as a function of the compression force, f_c. The diamonds indicate W and γ calculated with the Simson model for the smallest compression (the first cycle) [9,10].

rupture force in Figure 2. In Figure 4 we show W and γ as a function of the initial force applied to the vesicle during unbinding. It is clear that the adhesion energy and membrane tension obtained at the point of rupture validates the dynamical measurements, with the dynamical approach having the advantage of being able to monitor these quantities during the entire measurement.

In order to further validate our experimental approach, a model developed by Simson and coworkers, coupled with the Young-Dupré equation, was compared to the results in Figure 4 [9,10]. The Simpson model is convenient as it provides a simple analytical solution for the dynamic measurements with the assumption of a small deformation (nearly spherical cell). As expected, we found that W obtained with the Simson model was in agreement with other approaches for the smallest deformation where the model assumptions are valid (see Fig. 4).

3.2 Adhesion and membrane tension of living cells

In order to illustrate the value of the dynamical MD approach, we have carried out measurements on *living* HeLa cells adhering to a gold substrate. Prior to experiment, cells were detached from the culture dish (with trypsin) and resuspended in media (α-MeM with 10% fetal bovine serum) before being transferred into the experimental chamber. The cells studied had a diameter ranging from 15 to 25 μm. In Figure 5a we show the results of 4 push/pull cycles, with a substrate velocity of 0.5 μm/s, where the cell is compressed to the same extent in each cycle. Clearly visible in each cycle is 1): the push of the cell into the substrate; 2): a subsequent relaxation of the cell as it responds to the substrate which remains stationary; 3): the unloading of the cell; and finally 4): the rupture of the cell from the substrate. As before, the rupture force can be used to evaluate the adhesion energy, W, and likewise we can apply the BWdG model to the dynamic data under tension. Surprisingly the simple membrane model of BWdG, provides excellent agreement with rupture force

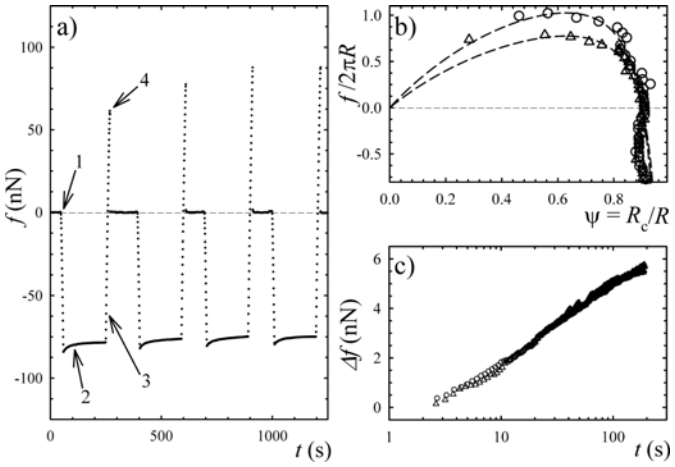

Fig. 5. a) Adhesion measurement cycles for living HeLa cells. b) Fit of the BWdG model during unbinding to the first two cycles. From the rupture point one obtains $W_1 = 1.47\,\mathrm{nN}/\mu\mathrm{m}$ and $W_2 = 1.99\,\mathrm{nN}/\mu\mathrm{m}$ while the dynamic model yields $W_1 = 1.55\,\mathrm{nN}/\mu\mathrm{m}$, $\gamma_1 = 2.73\,\mathrm{nN}/\mu\mathrm{m}$, $W_2 = 2.05\,\mathrm{nN}/\mu\mathrm{m}$, and $\gamma_2 = 3.62\,\mathrm{nN}/\mu\mathrm{m}$. c) Logarithmic relaxation during compression for the first two cycles. For clarity only cycle 1 (triangles) and cycle 2 (circles) are shown in b) and c).

measurements (see Fig. 5b) for the living cell. W is found to be about an order of magnitude larger for the living cells, which have binding proteins, than simple lipid vesicles. Interestingly, the agreement between the model and the data is systematically off under compression of the cell (note the fit for negative values of $f/2\pi R$), but in excellent agreement when the cell is pulled from the surface. We suspect that this is due to the active response of the living cell to the perturbation, an observation that is consistent with the relaxation processes observed under compression (see label 2 in Fig. 5a). The relaxation data is of sufficient quality to rule out a simple exponential response, rather, the measured response of the cell to a stress is consistent with a slow *logarithmic relaxation* process, $f \sim \ln(t)$, as shown in the inset of Figure 5c. Logarithmic relaxation is seen in strongly interacting complex systems such as granular materials, spin-glasses, and proteins [17].

4 Conclusions

Here we have presented a novel MD measurement which is unique because the force, displacements and the contact area are known at every measurement point. As a result, the dynamics of adhesion and elasticity are readily accessible using various theoretical models. Our approach to studying the mechanical properties of cells is simple, versatile, and direct, since the pipette acts as a force transducer. Furthermore, the stiffness of the transducer can easily be adapted by changing the dimensions of the pipette. We have carried out measurements on vesicles and living cells adhering to a gold substrate. The use of vesicles has enabled us to establish the validity of the technique because comparison could be made with models. The study of the living cells has the potential to elucidate biological

processes. Under tension, the cells were well fit by a model developed by Brochard-Wyart and de Gennes. Interestingly, deviation from the model was observed for compression of the cells. This rich behavior may be linked to the observation of a logarithmic relaxation mechanism under the external stress. The MD methodology has the potential to be applied to a wide variety of systems such as: specific or non-specific adhesion on various substrates (cell-cell or cell-substrate); the mechanical response of living cells to changes in their environment (*i.e.* membrane tension, contractile forces, drugs); and other systems that can be manipulated with the micropipette like colloids, fibers, microtubules, and aggregates. Furthermore, by scanning a sample it is possible to carry out friction measurements as well as imaging.

The authors thank Profs. R. Epand, and J. Forrest for valuable discussions, and Prof. R. Pelton for discussions and the generous loan of some equipment. Financial support from NSERC and AFMnet of Canada is gratefully acknowledged.

References

1. M.M. Stevens, J.H. George, Science **310**, 1135 (2005).
2. P. Carmeliet, R.K. Jain, Nature **407**, 249 (2002).
3. G. Christofori, Nature **441**, 444 (2006).
4. E.A. Evans, Biophys. J. **31**, 425 (1980).
5. E.A. Evans, D. Needham, Macromolecules **21**, 1822 (1988).
6. E.A. Evans, Colloids Surf. **43**, 327 (1990).
7. E.A. Evans *et al.*, Biophys. J. **59**, 849 (1991).
8. E.A. Evans *et al.*, Biophys. J. **65**, 2580 (1995).
9. D.A. Simson *et al.*, Biophys. J. **74**, 2080 (1998).
10. V. Heinrich, C. Ounkomol, Biophys. J. **93**, 363 (2007).
11. F. Brochard-Wyart, P.-G. de Gennes, C. R. Phys. **4**, 281 (2003).
12. S. Pierrat *et al.*, Biophys. J. **87**, 2855 (2004).
13. A. Yeung *et al.*, J. Colloid Interface Sci. **196**, 113 (1997).
14. G.W. Francis *et al.*, J. Cell Sci. **87**, 519 (1987).
15. D.S. Dimitrov, M.I. Angelova, Bioelectroch. Bioenerg. **19**, 323 (1988).
16. Y.-S. Chu *et al.*, Phys. Rev. Lett. **94**, 028102 (2005).
17. J.J. Brey, A. Prados, Phys. Rev. E. **63**, 021108 (2001).